Journal of Photochemistry and Photobiology A: Chemistry 356 (2018) 38–45

Contents lists available at ScienceDirect

Journal of Photochemistry and Photobiology A: Chemistry

journal homepage: www.elsevier.com/locate/jphotochem

FeO_x,SiO_2,TiO_2/Ti composites prepared using plasma electrolytic oxidation as photo-Fenton-like catalysts for phenol degradation

M.S. Vasilyeva[a,b], V.S. Rudnev[a,b,*], A.A. Zvereva[a,b], A.Yu. Ustinov[a,b], O.D. Arefieva[a], V.G. Kuryavyi[a,b], G.A. Zverev[b]

[a] Far Eastern Federal University, Vladivostok, Russia
[b] Institute of Chemistry, Far Eastern Branch, Russian Academy of Sciences, Vladivostok, Russia

ARTICLE INFO

Article history:
Received 7 November 2017
Received in revised form 30 November 2017
Accepted 5 December 2017
Available online 14 December 2017

Keywords:
Fe-containing oxide coatings
Surface composition
Phenol photodegradation
Reaction mechanism

ABSTRACT

FeO_x,SiO_2,TiO_2/Ti composites were formed through combination of the methods of plasma electrolytic oxidation and impregnation. The coatings have been studied by the methods of X-ray diffraction analysis, electron microscopy, and X-ray photoelectron and IR spectroscopy. The photocatalytic activity of oxide coatings has been investigated in the phenol degradation reaction. It was shown that the Fe-containing oxide coatings were highly active in the phenol decomposition under the following conditions: 1. the presence of hydrogen peroxide; 2. ultraviolet irradiation; 3. the presence of iron hydroxide on the surface of coatings. The results suggest that the catalysts studied are similar to photo-Fenton-like catalysts in their mechanism of action. Their activity is determined by the formation of iron-peroxide complexes fixed on the coating surface and thereafter of active radicals under the UV irradiation. The kinetics of phenol decomposition and the effect of the solution pH on the phenol decomposition degree has been studied.

1. Introduction

Presently, contamination of objects by wastewaters containing stable high-toxicity contaminants constitutes an urgent problem. In view of this, a substantial practical interest is concerned with development of efficient and reliable methods of these contaminants destruction. The most promising technologies of destruction of a broad range of toxic chemicals are those of nonchemical treatment based on Advanced Oxidation Processes (AOPs) [1]. These processes include the formation of high-reactivity hydroxyl radical ($HO^{\bullet}$) – one of the strongest oxidation agents [2].

Among different AOPs, the Fenton reaction is one of the most powerful oxidation processes of destruction of stable organic contaminants [3–5]. In the homogeneous Fenton process, the formation of hydroxyl radicals ($HO^{\bullet}$) occurs as a result of the catalytic decomposition of H_2O_2 in the acidic medium (pH 2.8–4.0) in the presence of Fe^{2+} ions [5]:

$$Fe^{2+} + H_2O_2 \rightarrow Fe^{3+} + HO^- + HO^{\bullet} \quad (1)$$

According to [6–10], the Fenton process rate increases significantly under effect of visible or ultraviolet radiation due to decomposition of photoactive $Fe(OH)^{2+}$ particles, thus promoting extra generation of $HO^{\bullet}$ radicals in solution:

$$Fe\ (OH)^{2+} + h\nu \rightarrow Fe^{2+} + HO^{\bullet} \quad (2)$$

However, the conventional homogeneous Fenton process has a number of disadvantages, in particular, the use of substantial amounts of iron in the soluble form, which must be removed upon the process completion [11]. To overcome this problem, one can use heterogeneous Fenton-like catalysts prepared through deposition of iron oxide on solid substrates, such as synthetic and natural zeolites [12], laterite [13], clays [14–17], and silica [18].

A special interest is associated with FeO_x/SiO_2 composites, since iron oxides are characterized with strong affinity to silica and can be deposited directly on the amorphous silica [19]. In view of this, the synthesis conditions and properties of FeO_x/SiO_2 composites are under intensive research [20–25].

Oxide coatings deposited on metallic substrates can be of certain interest as heterogeneous catalysts [24,26–42]. The advantages of such composites include the increased thermal and mechanical stability, high electric and thermal conductivity, relatively low cost, and the possibility to produce articles of complex geometric shapes.

* Corresponding author at: Institute of Chemistry, Far Eastern Branch, Russian Academy of Sciences, Vladivostok, Russia.
E-mail address: rudnevvs@ich.dvo.ru (V.S. Rudnev).

https://doi.org/10.1016/j.jphotochem.2017.12.007
1010-6030/

One of the methods, which allows technologically sound formation of multicomponent oxide coatings on metals, is plasma electrolytic oxidation (PEO) – the creation of oxide layers on metals under effect of spark and arc discharges at the metal/electrolyte interface [43,44]. The formed composites can be used as catalytically active compounds supports [26–33], catalysts [32–34], and photocatalysts [24,35–41] of various chemical processes. In particular, Fe-containing oxide layers on titanium formed by the PEO method are studied as photocatalysts of dyes degradation [41], while those on titanium and carbon steel of the Q235 grade – as heterogeneous Fenton-like catalysis of phenol degradation [24,35,36].

FeO_x/SiO_2 composites promising for application as heterogeneous Fenton-like catalysts can be fabricated as by the single-stage PEO method in silicate electrolytes with additives of iron compounds [24] as by impregnation of SiO_2,TiO_2/Ti composites formed by the PEO method in silicate electrolytes in iron salts solutions [31]. In the latter case, it is possible to obtain oxide layers with higher content of a transition metal manifesting higher catalytic activity in CO oxidation, as compared to oxide layers formed by the single-stage PEO method [32]. In SiO_2,TiO_2 oxide layers, silicon is concentrated in the coatings external parts as an amorphous silica characterized with high porosity and humidity absorption [28,45].

In view of the above, the objective of the present work consisted in studies of the activity of Fe-containing composites fabricated through combination of PEO and impregnation methods with subsequent annealing in the reaction of phenol degradation under ultraviolet radiation in the presence of hydrogen peroxide.

2. Materials and methods

2.1. Samples preparation

Electrodes for plasma electrolytic oxidation were produced from sheet titanium of the VT1-0 grade as plates of a size of $2.0 \times 2.0 \times 0.1$ cm^2. Samples were chemically polished in a mixture of concentrated acids HF:HNO_3 = 1:3 at 60 – 80°C for 2–3 s and washed in distilled water.

For solutions preparation, commercial reagents ($Na_2SiO_3 \cdot 5H_2O$ of the analytical grade and $Fe(NO_3)_3$ of the chemically pure grade) and distilled water were used.

Silicon oxide layers on titanium (SiO_2,TiO_2/Ti) were formed within 10 min in the galvanostatic mode at an effective current density of 0.1 A/cm^2 on anode-polarized titanium in 0.1 M aqueous electrolyte Na_2SiO_3. A TER4–63/460R–2–2–UKhL4 thyristor device with the unipolar current waveform was used as a current source. The process was carried out in a vessel made of heat-resistant glass of a volume of 1000 mL. The cathode comprised a tubular coil made of stainless steel of the Kh18N9T grade cooled by tap water. The oxidized samples were washed with distilled water and dried in air.

The fabricated SiO_2,TiO_2/Ti composites were immersed for 1 h into an aqueous solution containing 1 mol/L $Fe(NO_3)_3$, after which the remained solution was removed by filtering paper and the samples were dried over the stove and annealed for 4 h in a muffle furnace in air at temperatures from 100 to 750 °C.

2.2. Structure and composition characterization

The samples phase compositions were determined by the method of X-ray diffraction analysis using a D8 ADVANCE diffractometer (Germany) in Cuk$_\alpha$-radiation in accordance with a standard technique. Identification of compounds contained in the samples under study was performed in an automatic EVA search mode using the PDF–2 database.

The surface morphology was studied using a Hitachi S-3400 high-resolution scanning electron microscope (SEM) with an Ultra Dry energy-dispersive spectrometer (Thermo Scientific, USA) and a SUPERPROBE JXA-8100 microprobe X-ray spectral analyzer (JEOL, Japan).

To determine the element composition of the oxide coating surface, the method of X-ray photoelectron spectroscopy (XPS) was used. Measurements of X-ray photoelectron spectra were carried out using a Specs superhigh-vacuum device (Germany) with 150-mm hemispheric electrostatic analyzer. MgK_α-radiation was used for ionization. The depth of the analyzed surface layer was about 3 nm. To remove the upper layer, etching by Ar^+ ions was used (energy 5000 eV, scanning time 5 min, etching rate ~0.1 Å/s). The spectra calibration was performed on C1s-lines of hydrocarbons with the energy that was stated to be equal to 285.0 eV.

IR spectra were recorded using a TENSOR 27 Fourier IR spectrometer (Bruker, Germany). A drop of Vaseline was put on the PEO sample. The Vaseline-wetted area was peeled by a scalpel on a KBr glass, which was then placed into the spectrometer inside the sample holder.

2.3. Photocatalytic studies

The photocatalytic activity of the fabricated samples was determined through photodegradation of phenol in an aqueous solution (pH 3–7, 50 mg/L) containing 10 mmol/L H_2O_2 under ultraviolet radiation. To attain pH 3 or 4, the phenol solution with pH 5 was added with a certain amount of H_2SO_4, for pH 6 и 7–NaOH. Total phenols content in the solutions under study was determined by the spectrophotometry method in accordance with the Folin–Ciocalteu method [46].

A UV-mini 1240 spectrophotometer (Shimadzu, Japan) was used to measure concentration changes using the Bouguer–Lambert–Beer equation: $A = \varepsilon \times l \times C$, where A, ε, l, and C – the solution optic density, the molar absorption coefficient, the beam path length, and the solution concentration, respectively. Since ε and l are constants, C is directly proportional to the optic density and can be obtained by measuring the parameter A.

For photocatalytic studies, 100 mL of phenol solution with hydrogen peroxide and a sample of a size of 20 × 20 mm used as a photocatalyst were placed into a quartz cell. An SB-100P UV-lamp (radiation maximum at a wavelength of 365 nm) was used as a radiation source. In each experiment, prior to radiation, the solution with a sample inside it was left in darkness for 30 min to establish the adsorption/desorption equilibrium, after which the solution optic density was measured – it was used as a reference point A_0. Thereafter, the sample inside the solution was UV-irradiated for different time periods – from 30 to 300 min.

To determine the phenol content, 50 mL of the studied solution diluted in 10 times was added with 1 mL of the Folin–Ciocalteu's reagent and 1.5 mL of 20% solution of Na_2CO_3. The obtained mixture was stirred for 30 min for color development. The optic density measurement was carried out at λ = 700 nm. The degree of phenol degradation was calculated according to the formula

$$X = (A_0 - A)/A_0 \times 100\%, \quad (3)$$

where A – the solution optic density upon irradiation, A_0 – that prior to irradiation upon holding in darkness with the sample for 30 min.

Total concentration of the dissolved iron after photocatalytic tests, including the sample holding in phenol aqueous solution with hydrogen peroxide for 30 min and subsequent irradiation for 2 h, was determined by the spectrophotometry method using 1,10-phenanthroline (FerroVer method) and a UV–vis DR 2800 spectrophotometer (Hach Lange, USA).

3. Results and discussion

3.1. Oxide coatings characterization

Fig. 1 and Table 1 show the phase composition data for Fe-containing oxide layers on titanium fabricated through combination of the methods of PEO and impregnation that underwent extra thermal treatment at different temperatures. The X-ray image of the coating annealed at 100 °C contains reflections assigned to titanium oxide in rutile and anatase modifications and small peaks corresponding to FeOOH (Fig. 1a). The coatings annealed at 200 °C have the same phase composition as at 100 °C (Table 1). On the X-ray image of the coating annealed at 300 °C, one observes traces (on those of the coating annealed at 400 °C – small reflections) assigned to α-Fe_2O_3 (Fig. 1b), which increase along with the increase of the annealing temperature up to 700 °C (Fig. 1c). In other words, the FeOOH transformation into hematite occurs at temperatures above 200 °C, which is in agreement with the literature data [47].

Table 1
Phase and element composition data

Annealing temperature, °C	Phase composition
100	TiO_2 (anatase, rutile), FeOOH (traces)
200	TiO_2 (anatase, rutile), FeOOH (traces)
300	TiO_2 (anatase, rutile), α-Fe_2O_3 (traces)
400	TiO_2 (anatase, rutile), α-Fe_2O_3
500	TiO_2 (anatase, rutile), α-Fe_2O_3
600	TiO_2 (anatase, rutile), α-Fe_2O_3
700	TiO_2 (anatase, rutile), α-Fe_2O_3
750	TiO_2 (anatase, rutile), α-Fe_2O_3

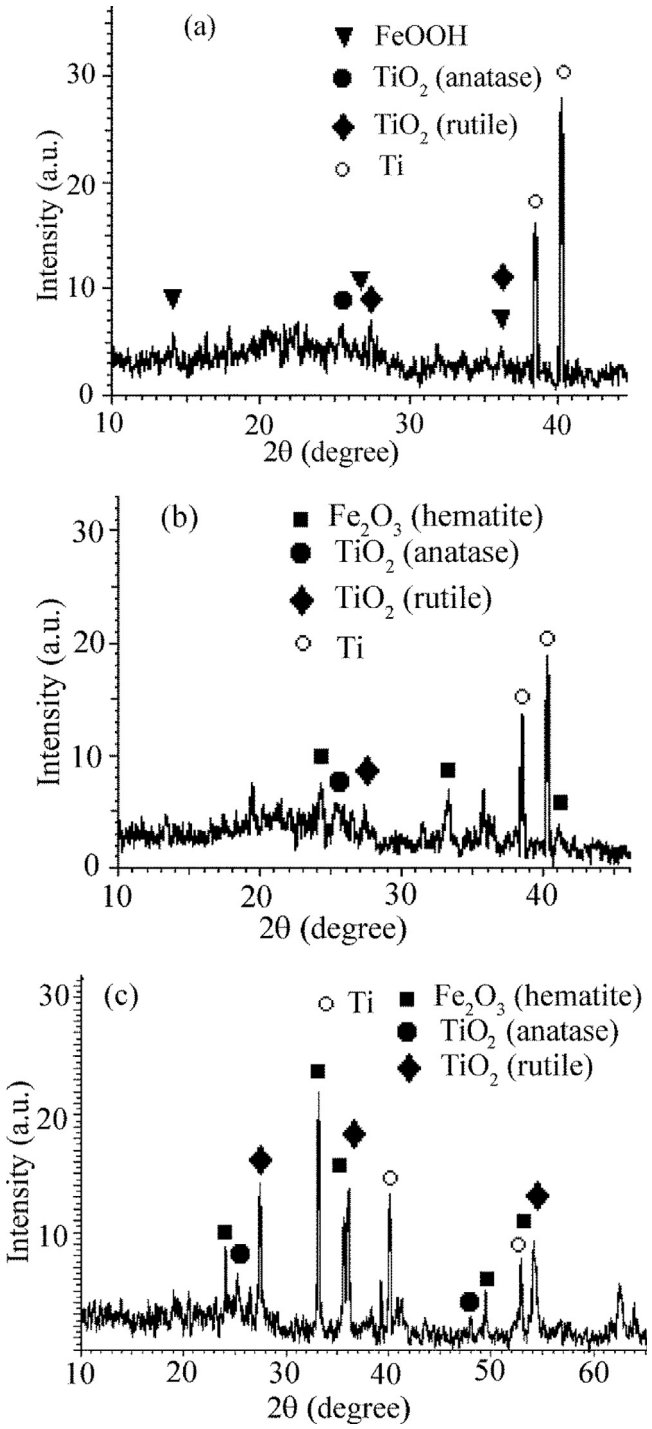

Fig. 1. X-ray diffraction patterns for FeO_x,SiO_2 composite annealed at temperatures, °C: a – 100; b – 400; c – 700.

Fig. 2 shows the IR spectra of iron-containing oxide layers on titanium annealed at 100 and 500 °C. The IR spectrum of the sample annealed at 100 °C contains bands at 1091 and 468 cm^{-1} corresponding to vibrations of Si—O—Si groups. The range of Si—O—Si bonds vibrations around 1090 cm^{-1} can include superposition with those of Me—OH bonds (Me – metal) [48]. That is why the band at 1091 cm^{-1} can include the signal from Fe—OH.

The IR spectrum of the sample annealed at 500 °C contains bands at 1050, 520, and 460 cm^{-1}. The band at 1050 cm^{-1} could correspond to stretching vibrations of Si—O—Si groups. This band is shifted relatively to similar one in the sample annealed at 100 °C. Such a shift can be explained by disappearance of Fe—OH bonds, whose vibration frequency is similar to that of Si—O—Si bonds. The bands at 520 and 460 cm^{-1} characterize iron oxide in the hematite modification [49]. The IR spectroscopy data corroborate the XRD results.

According to the data of X-ray spectral element analysis, all the coatings under study (the analyzed layer depth ~1–2 μm) contain iron, silicon, and oxygen, whose concentration dependencies on temperature are shown in Fig. 3. The highest contents of iron (~37 at.%) and oxygen (~51 at.%) and the lowest content of silicon (~12 at.%) were found in oxide layers annealed at 100 °C (Fig. 3). In oxide layers annealed at 200 °C and higher, the iron content decreases by 5–10 at.% in average, the oxygen content – by 1–4 at.%, whereas the silicon content in such layers increases by 7–10 at.%. Besides, the coatings annealed at 100 and 200 °C do not contain titanium, which was found in quantities of 1–3 at.% in coatings annealed at 300 °C and higher (Fig. 3). Changes in the element composition correlate to changes in the surface structure (Fig. 4).

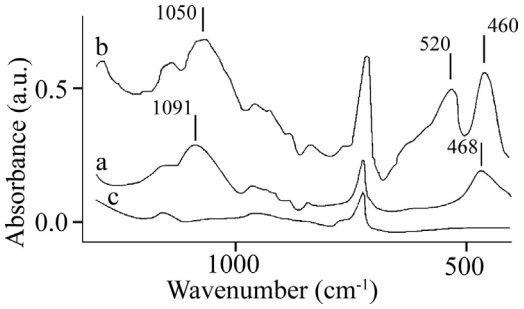

Fig. 2. IR spectra of Fe-containing layers on titanium annealed at 100 °C (a) and 500 °C (b). (c) – Vaseline spectrum.

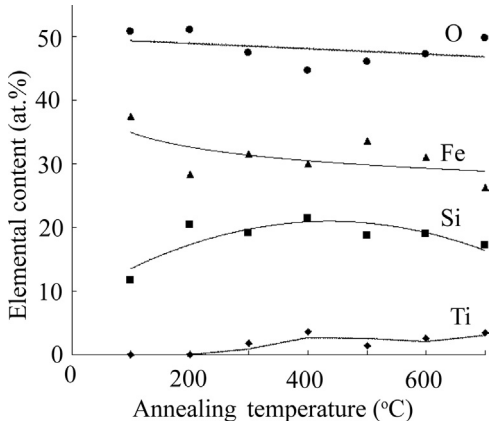

Fig. 3. The elemental content for FeO_x,SiO_2 compositions in dependence on annealing temperature (from the XSA data).

As can be concluded from SEM images of Fe-containing coatings annealed at different temperatures (Fig. 4), the surfaces of all the coatings were heterogeneous with high degree of roughness and the presence of numerous coral-like structures, which generally characterizes coatings formed in the silicate electrolyte [32]. At the annealing temperature near or higher than 200 °C, there occurs, as seen from above data of IR spectroscopy and X-ray diffraction analysis, the FeOOH decomposition until Fe_2O_3 and H_2O (with evaporation), which is accompanied with contraction and cracking of initially virtually solid hydrated iron-containing layer deposited through impregnation. Thereafter, the element composition of the coating external layer stabilizes. Finding titanium at the annealing temperature above 200 °C must be related to the emergence and development of cracks (Fig. 4) and the contribution of the opened parts of the TiO_2-containing initial coating into the composition to be determined.

Table 2 and Fig. 5 show the data of X-ray photoelectron spectroscopy used to analyze the surface layer of a thickness of

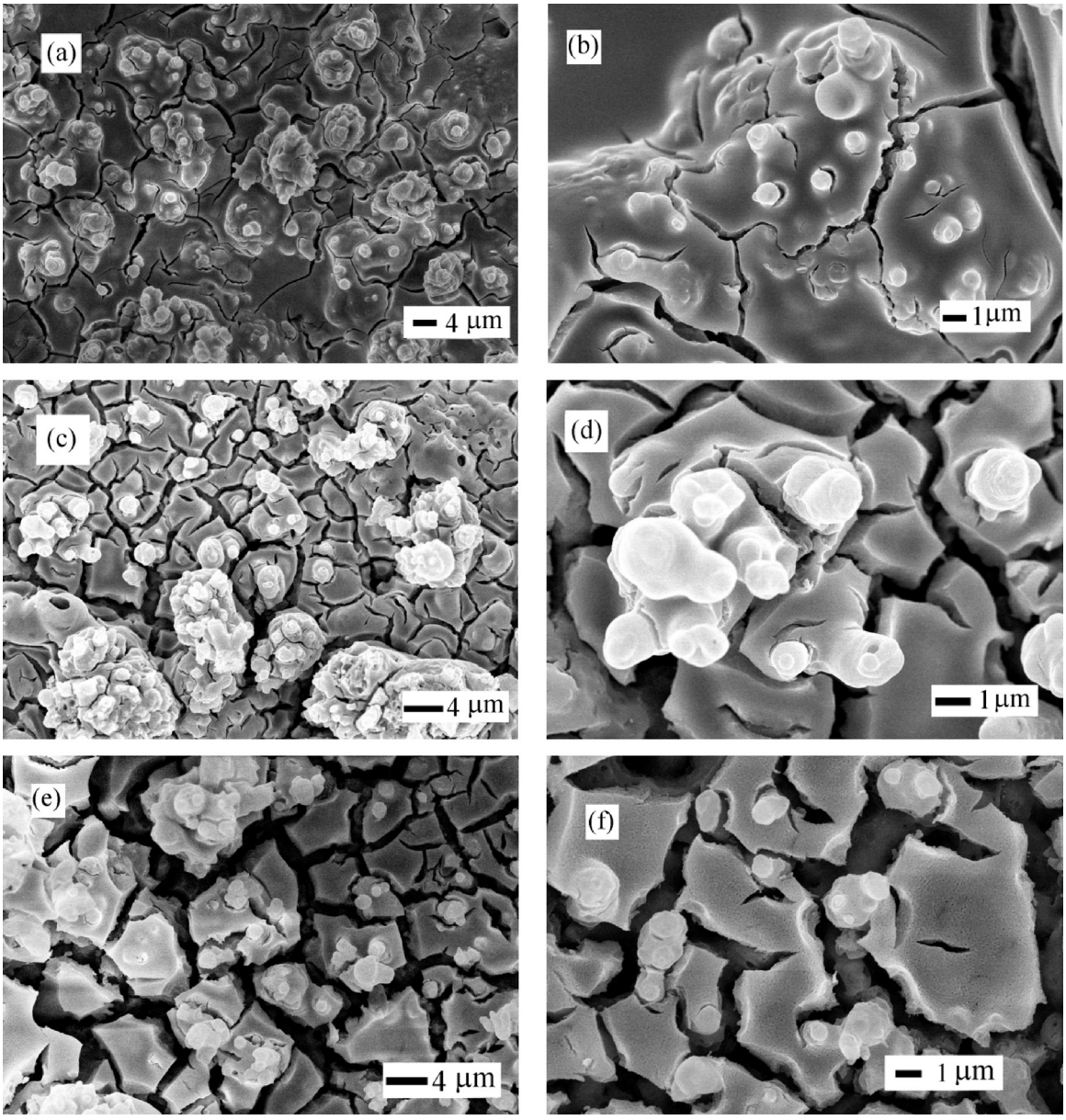

Fig. 4. SEM images of the surfaces of samples annealed at different temperatures, °C: a, b – 100; c, d – 400; e, f – 500.

Table 2
Binding energies (eV) and elemental content (at.%) in the studied samples from XPS data, in the numerator – before etching, in the denominator – after etching.

Element	Sample annealing temperature, °C					
	100		300		100	300
	Surface chemical composition					
	E_b (eV)	C (at. %)	E_b (eV)	C (at. %)	Chemical groups or compounds	
Fe (2p)	711.8 710.8	4.1 16.1	711.2 710.3	11.7 23.0	FeOOH FeO	Fe_2O_3 FeO
O (1s)	No signal 534.5	0.0 11.3	533.6 533.9	13.1 10.1	NO_x	
	532.5 532.2	27.6 11.9	531.9 532.0	10.7 7.6	SiO_2, -CO_x	
	530.4 530.0	14.8 33.3	530.1 530.0	35.7 32.9	FeO_x	
Si (2p)	104.0 104.8	7.4 10.9	104.1 104.4	9.4 10.2	SiO_2	
C (1s)	No signal 289.4	0.0 1.4	289.0 289.2	2.1 1.3	-COO	
	288.2 287.4	3.5 2.4	287.2 286.9	1.7 2.2	-CO	
	285.0 285.0	39.9 10.2	285.0 285.0	15.6 10.5	-CC	
N (1s)	407.0 403.1	2.7 2.5	No signal 399.0	0.0 2.2	NO_x, N_2	

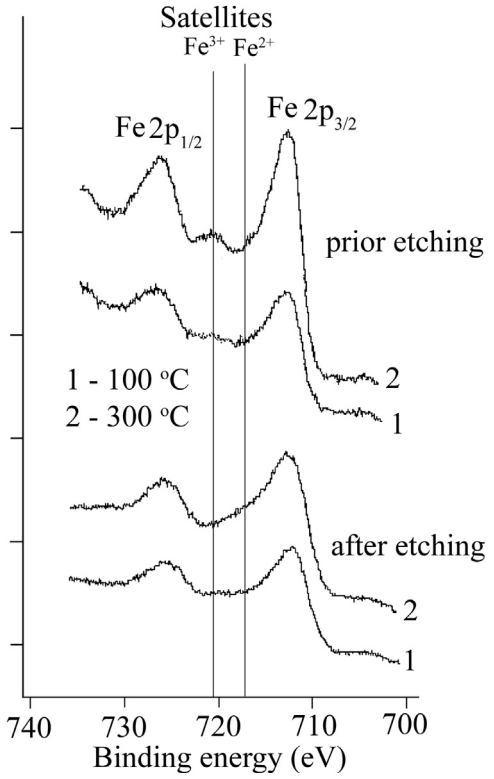

Fig. 5. Fe $2p_{1/2}$ and Fe $2p_{3/2}$ XPS spectra of oxide layers on titanium annealed at different temperatures.

~3 nm. According to the XPS data, the surface layer of samples annealed at 100 and 300 °C contains iron, silicon, oxygen, carbon, and nitrogen (Table 2). Similarly to the XSA data, titanium was not found in surface layers of the studied samples, which indicates to the fact that they consist mainly of compounds of electrolyte elements and impregnation solution and do not contain the titanium base material.

In accordance with the XPS data (analysis depth ~3 nm), in the composition of the surface layer of the sample annealed at 100 °C, the iron content is 4.1 at.%. In the subsurface layer of the same sample (upon etching of the upper layer of a thickness of ~3 nm), the iron content increases 4-fold. In the surface layer of the sample annealed at 300 °C, the iron content is 11.7 at.%, whereas in the subsurface layer it increases 2-fold. Thus, for two samples annealed at different temperatures, one observes a substantial increase of the iron content along with the increase of the coating depth and, therefore, the presented data do not contradict the XSA data providing higher iron contents. Analysis of the XPS spectra (Fig. 5) indicates that iron in the surface layer of the sample annealed at 100 °C is present in the oxidation state of +3, probably, in the form of FeOOH characterized with the binding energy (E_b) $Fe2p_{3/2}$ about 711.5 eV. Besides, the presence of Fe_2O_3 (from literature data, the average E_b $Fe2p_{3/2}$ ~711.2 eV). Possibly, a small part of iron is present in the form of nitrate, since one observes a substantial increase of the content of the metal-oxide oxygen over that of iron (Table 2). In the subsurface layer (upon etching by ion bombardment of the layer of a thickness of a few nm), the iron state changes significantly: E_b decreases down to 710.8 eV, the shake-up-satellite shifts to the side of $2p_{3/2}$ band, which indicates to the presence of Fe^{2+}. One must not exclude that these changes are induced by the effect of high-energy argon used for etching.

In the sample annealed at 300 °C, iron is present predominantly in the form of Fe_2O_3 (Fig. 4, Table 2).

The above peculiarities correlate to the oxygen state and content. In the upper layer of the sample annealed at 100 °C, one observes three types of oxygen – bound to nitrogen, contained in SiO_2 and metal-oxide ones. The contents of oxygen forms are in agreement with those of silicon and iron.

3.2. Photocatalytic activity of the samples under study

Preliminary tests demonstrated that phenol degradation did not occur: a) in the absence of PEO-coatings; b) on SiO_2,TiO_2/Ti composites not modified with iron; c) in the absence of hydrogen peroxide in solution; d) without application of UV irradiation on the solution. In other words, the process of phenol decomposition occurs only in the presence of an iron-containing sample, hydrogen peroxide, and UV radiation. Therefore, one can assume that the reaction of formation of radicals responsible for phenol decomposition proceeds through formation of hydroperoxide surface

complexes PEO = Fe^{3+} – $OH(H_2O_2)_s$ in accordance with the mechanism suggested in [50] for the heterogeneous Fenton-like catalysis:

$$PEO = Fe^{3+} - OH + H_2O_2 \rightarrow PEO = Fe^{3+} - OH(H_2O_2)_s \quad (4)$$

$$PEO = Fe^{3+} - OH(H_2O_2)_s + h\nu \rightarrow PEO = Fe^{2+} + {}^{\bullet}O_2H + H_2O \quad (5)$$

$$O_2H \leftrightarrow H^+ + {}^{\bullet}O_2^- \quad (6)$$

$$PEO = Fe^{3+} - OH(H_2O_2)_s + {}^{\bullet}O_2H/{}^{\bullet}O_2^- \rightarrow PEO = Fe^{3+} - OH + H_2O/OH^- + {}^{\bullet}OH + O_2 \quad (7)$$

$$PEO = Fe^{2+} + H_2O_2 \rightarrow PEO = Fe^{3+} - OH + {}^{\bullet}OH + H_2O \quad (8)$$

Besides, additional formation of hydroxyl radicals is possible through that of unstable surface complexes PEO = Fe^{4+} = O in accordance with the mechanism [50]:

$$PEO = Fe^{3+} - OH + h\nu \rightarrow PEO = Fe^{4+} = O + HO^{\bullet} \quad (9)$$

$$PEO = Fe^{4+} = O + H_2O \rightarrow PEO = Fe^{3+} - OH + HO^{\bullet} \quad (10)$$

Comparison of the photocatalytic activity of iron-containing samples annealed at different temperatures was performed under identical conditions: 50 mL of phenol solution (C = 50 mg/L), irradiation time 2 h, pH = 3, C(H_2O_2) = 10 mmol.

According to the obtained results, the degree of phenol degradation depends on the samples annealing temperature (Fig. 6). At using iron-containing oxide layers annealed at 100 and 200 °C as photocatalysts, this parameter attains more than 88%. However, for samples annealed at 300 °C, the degree of phenol degradation decreases more than 2-fold (Fig. 6).

Probably, such a difference in photocatalytic activity of samples annealed at different temperature is caused by the difference in their surface composition.

According to the XRD, IR spectroscopy, and XPS data, the surface of coatings annealed at 100 and 200 °C contain iron metahydroxide that transforms to hematite (α-Fe_2O_3) along with the temperature increase. Hematite and FeOOH comprise semiconductors of the *n*-type with small widths of the forbidden band equal to ~2.2 and ~2.1 eV, respectively [47]. However, their application as photocatalysts is limited due to high rate of electrons and holes recombination [47,51,52].

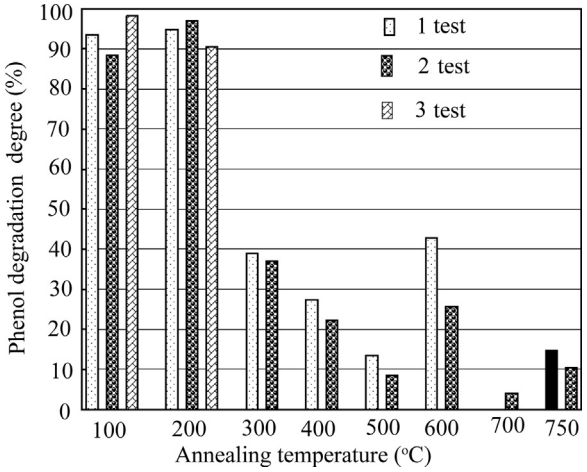

Fig. 6. Dependence of the degradation degree on the sample annealing temperature.

In our case, at the conditions of UV irradiation, the samples under study are not active in phenol degradation in the absence of hydrogen peroxide. The latter could be caused by the fact that hydrogen peroxide has the role of a scavenger in Fenton-like processes, i.e., it serves as a trap and could significantly reduce the rate of electrons and holes recombination [52].

The fact that the samples activity decreases at the FeOOH substitution by α-Fe_2O_3 in them can be explained by dehydroxylation of the samples surface along with the increase of their annealing temperature, i.e., the decrease of the number of hydroxyl groups Fe-OH participating in the photocatalytic reaction. Besides, hydroxyl groups bound to one iron atom (mono-coordinated groups), which are more reactive in comparison with two- and three-coordinated ones, can be predominant in the goethite structure [47].

The authors of [53] explained higher activity of goethite in comparison to that of hematite by higher goethite dissolution and, as a result, a substantial contribution of the homogeneous Fenton-process (reactions 1, 2) into total process of hydroxyl radicals' formation. However, as was shown in our studies, the iron concentration in phenol solution upon photocatalytic tests depended insignificantly on the studied sample and experimental conditions (Table 3). Therefore, the dissolved iron does not have a determining effect on the degree of phenol degradation in the presence of samples annealed at different temperatures.

In addition, one must not exclude changes in the surface morphology on the degree of phenol degradation. The increase of the number and sizes of cracks formed at samples annealing (Fig. 4) could result in diffusion slowdown related to penetration and delay of the studied phenol solution in PEO-coatings cracks.

3.3. Dependence of the phenol degradation degree on the reaction time

It was also established that phenol degradation depended on the irradiation time (Fig. 7). For example, in case of the sample annealed at 300 °C, the phenol degradation within first 60 min of irradiation does not occur. The phenol degradation degree for such a sample attains 36% within 2 h and increases up to 92% within 3 h. Thereafter, it changes insignificantly (up to 95%) along with the increase of the irradiation time from 3 to 5 h.

At the same time, in case of the sample annealed at 100 °C, the degradation degree within 60 min of irradiation is already equal to 67%, while upon 90 min it attains 96% and, thereafter, changes insignificantly.

The latter enables assuming that slow stages related to radicals formation take place before the start of the active phenol degradation stage.

According to [50], the formation of hydroperoxide surface complexes between hydrogen peroxide and Fe(III) active centers on the surface is an initiating stage of total Fenton-like process (Eq. (4)). In view of the fact that in our case phenol degradation does not occur in the darkness and in the absence of hydrogen peroxide, the formation of surface PEO = $Fe^{III}OH(H_2O_2)_s$ complexes must be the limiting, very slow stage (Eq. (4)). Then, along with

Table 3
Iron concentration in phenol solution upon photocatalytic tests under different conditions.

Annealing temperature, °C	pH	C (iron), mg/L
100	3.05	0.26
300	3.02	0.27
100	5.97	0.16
100	7.06	0.17

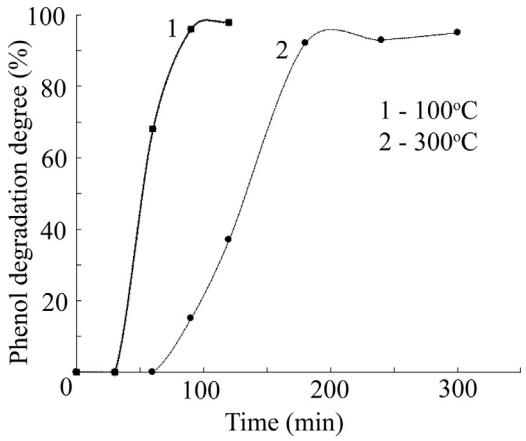

Fig. 7. Dependence of the degradation degree on the time of irradiation of samples annealed at different temperatures.

formation of surface complexes, their decomposition under UV irradiation, and accumulation of a critical amount of hydroxyl radicals in solution, the process of phenol degradation dramatically accelerates as a result of a combination of reactions (5)–(8) (Fig. 7).

The increase of the initial period duration (Fig. 5), when the phenol degradation is not observed, is determined by slower formation of surface complexes on coatings containing iron oxides, as compared to those with iron hydroxides.

3.4. Effect of pH on the phenol degradation degree

It is generally known that the efficiency of homogeneous and heterogeneous Fenton processes depends on pH [10,14,54–58]. Fenton reactions proceed at high rates in acidic media (pH 2.8–4.0). To decontaminate wastewater streams containing phenolic compounds, Fenton-like catalysts capable to function in a broad pH range are of interest.

The effect of pH on phenol degradation for the samples under study annealed at 100 and 200 °C was estimated in the pH range from 3 to 7 (Fig. 8). One can see that at pH 3, 4, and 6 the degree of phenol degradation is rather high and about the same. Its insignificant decrease occurs at pH 5, while more substantial one– at pH 7. Therefore, the PEO-coatings on titanium with iron hydroxide on the surface we fabricated can be used as heterogeneous Fenton-like catalysts in the pH range 3–6.

In general, the obtained results corroborate the fact that heterogeneous photo-Fenton-like processes can be implemented in a rather wide pH range, which is an advantage before conventional homogeneous ones.

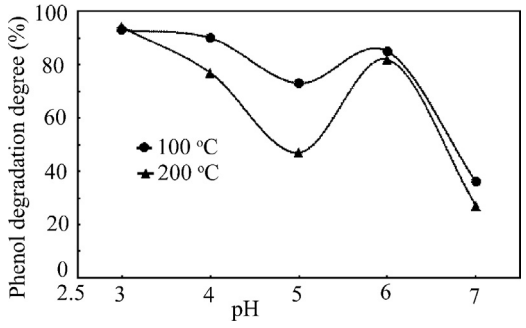

Fig. 8. Dependence of the degradation degree on the solution pH for the sample annealed at 100 °C.

4. Conclusions

The composition, surface structure, and photocatalytic activity in the reaction of phenol degradation of FeO_x,SiO_2,TiO_2/Ti composites formed by combination of the methods of plasma electrolytic oxidation and impregnation with subsequent annealing in air in the temperature range from 100 to 750 °C has been investigated. Oxide coatings annealed at 100 and 200 °C contain titanium oxide in anatase and rutile modifications and the crystalline phase FeOOH that transforms into hematite at higher temperatures. Photocatalytic activity of oxide coatings was studied in the reaction of phenol degradation under ultraviolet irradiation in the presence of hydrogen peroxide. The highest degree of phenol degradation (90% and higher) is attained in the presence of FeO_x, SiO_2,TiO_2/Ti composites that underwent thermal treatment at 100 and 200 °C. In the presence of samples annealed at higher temperatures, the degree of phenol degradation decreases several-fold. For the samples annealed at 100 and 200 °C, the degree of phenol degradation of >70% is attained in a rather wide pH range (3–6), which constitutes an advantage over the conventional homogeneous Fenton-like process.

The iron-containing oxide coatings on titanium fabricated and studied in the present work are promising for water decontamination from organic contaminants as Fenton-like heterogeneous photocatalysts.

Acknowledgments

The work was carried out within the State Order (project no. 265-2014-0001) and was partially supported by the FEBRAS Program of Basic Research “Far East” (project no. 265-20-15-0022). XPS data were obtained as part of the state assignment of the Russian Ministry of Education and Science, project No. 3.6478.2017/6.7.

References

[1] J.-M. Herrmann, C. Guillard, P. Pichat, Heterogeneous photocatalysis: an emerging technology for water treatment, Catal. Today 17 (1993) 7–20.
[2] A. Khataee, A. Naseri, M. Zarei, M. Safarpour, L. Moradkhannejhad, Chemometrics approach for determination and optimization of simultaneous photooxidative decolourization of a mixture of three textile dyes, Environ. Technol. 33 (2012) 2305–2317.
[3] A.R. Khataee, B. Vahid, B. Behjati, M. Safarpour, S.W. Joo, Kinetic modeling of a triarylmethane dye decolorization by photoelectro-Fenton process in a recirculating system: nonlinear regression analysis, Chem. Eng. Res. Des. 92 (2014) 362–367.
[4] S. Esplugas, J. Gi ménez, S. Contreras, E. Pascual, M. Rodríguez, Comparison of different advanced oxidation processes for phenol degradation, Water Res. 36 (2002) 1034–1042.
[5] C. Walling, A. Goosen, Mechanism of the ferric ion catalyzed decomposition of hydrogen peroxide. Effect of organic substrates, J. Am. Chem. Soc. 95 (1973) 2987–2991.
[6] V. Nadtochenko, J. Kiwi, Photolysis of FeOH2+ and FeCl2+ in aqueous solution. Photodissociation kinetics and quantum yields, Inorg. Chem. 37 (1998) 5233–5238.
[7] J. An, L. Zhu, Y. Zhang, H. Tang, Efficient visible light photo-Fenton-like degradation of organic pollutants using in situ surface-modified BiFeO3 as a catalyst, J. Environ. Sci. 25 (2013) 1213–1225.
[8] C.C. Amorim, M. Leão, R.F. Moreira, J.D. Fabris, A.B. Henriques, Performance of blast furnace waste for azo dye degradation through photo-Fenton-like processes, Chem. Eng. J. 224 (2013) 59–66.
[9] M.N. Chong, B. Jin, C.W.K. Chow, C. Saint, Recent developments in photocatalytic water treatment technology: a review, Water Res. 44 (2010) 2997–3027.
[10] F.L. Lam, X. Hu, A high performance bimetallic catalyst for photo-Fenton oxidation of Orange II over a wide pH range, Catal. Commun. 8 (2007) 2125–2129.
[11] J.A. Zazo, J.A. Casas, A.F. Mohedano, Chemical pathway and kinetics of phenol oxidation by Fenton’s reagent, Environ. Sci. Technol. 39 (2005) 9295–9302.
[12] D.J. Doocey, P.N. Sharratt, C.S. Cundy, R.J. Plaisted, Zeolite-mediated advanced oxidation of model chlorinated phenolic aqueous waste: part 2: solid phase catalysis, Process Saf. Environ. Prot. 82 (2004) 359–364.

[13] A. Khataee, F. Salahpour, M. Fathinia, B. Seyyedi, B. Vahid, Iron rich laterite soil with mesoporous structure for hetero-Fenton-like degradation of an azo dye under visible light, J. Ind. Eng. Chem. 26 (2015) 129–135.
[14] B. Iurascu, I. Siminiceanu, D. Vione, M.A. Vicente, A. Gil, Phenol degradation in water through a heterogeneous photo-Fenton process catalyzed by Fe-treated laponite, Water Res. 43 (2009) 1313–1322.
[15] Q. Chen, P. Wu, Z. Dang, N. Zhu, P. Li, J. Wu, X. Wang, Iron pillared vermiculite as a heterogeneous photo-Fenton catalyst for photocatalytic degradation of azo dye reactive brilliant orange X-GN, Sep. Purif. Technol. 71 (2010) 315–323.
[16] N. Platon, I. Siminiceanu, I.D. Nistor, N.D. Miron, G. Muntianu, A.M. Mares, Fe-pillared clay as an efficient Fenton-like heterogeneous catalyst for phenol degradation, Rev. Chim. (Bucharest) 62 (2011) 676–679.
[17] M. Idrissi, Y. Miyah, Y. Benjelloun, M. Chaouch, Degradation of crystal violet by heterogeneous Fenton-like reaction using Fe/Clay catalyst with H2O2, J. Mater. Environ. Sci. 7 (2016) 50–58.
[18] T. Liu, H. You, Q. Chen, Heterogeneous photo-Fenton degradation of polyacrylamide in aqueous solution over Fe(III)-SiO2 catalyst, J. Hazard. Mater. 162 (2009) 860–865.
[19] X. Xu, J. Wang, C. Yang, H. Wu, F.J. Yang, Sol–gel formation of γ-Fe2O3/SiO2 nanocomposites: effects of different iron raw material, J. Alloys Compd. 468 (2009) 414–420.
[20] M. Hosseinpour, Sh. Fatemi, S.J. Ahmadi, Catalytic cracking of petroleum vacuum residue in supercritical water media: impact of α-Fe2O3 in the form of free nanoparticles and silica-supported granules, Fuel 159 (2015) 538–549.
[21] F. Arena, G. Gatti, G. Martra, S. Coluccia, L. Stievano, L. Spadaro, P. Famulari, A. Parmaliana, Structure and reactivity in the selective oxidation of methane to formaldehyde of low-loaded FeOx/SiO2 catalysts, J. Catal. 231 (2005) 365–380.
[22] T. Meng, P. Xie, H. Qin, H. Liu, W. Hua, Xi Li, Zh. Ma, Fe2O3/SiO2 nanowires formed by hydrothermally transforming SiO2 spheres in the presence of Fe3+: Synthesis, characterization, and catalytic properties, J. Mol. Catal. A: Chem. 421 (2016) 109–116.
[23] S. Solinas, G. Piccaluga, M.P. Morales, C.J. Serna, Sol-Gel formation of γ-Fe2O3/SiO2 nanocomposites, Acta Mater. 49 (2001) 2805–2811.
[24] M.S. Vasilyeva, V.S. Rudnev, A.A. Zvereva, K.N. Kilin, A.A. Sergeev, K.A. Sergeeva, A.V. Nepomnyaschiy, S.S. Voznesenskiy, A.Yu. Ustinov, Characterization and photocatalytic activity of SiO2, FeOx coatings formed by plasma electrolytic oxidation of titanium, Surf. Coat. Technol. 307 (2016) 1310–1314.
[25] A. Jagminas, R. Ragalevičius, K. Mažeika, J. Reklaitis, V. Jasulaitienė, A. Selskis, D. Baltrūnas, A new strategy for fabrication Fe2O3/SiO2 composite coatings on the Ti substrate, J. Solid State Electrochem. 14 (2010) 271–277.
[26] Q. Luo, Q. Cai, X. Li, X. Chen, Characterization and photocatalytic activity of large-area single crystalline anatase TiO2 nanotube films hydrothermal synthesized on plasma electrolytic oxidation seed layers, J. Alloys Compd. 597 (2014) 101–109.
[27] S.F. Tikhov, G.V. Chernykh, V.A. Sadykov, A.N. Salanov, G.M. Alikina, S.V. Tsybuyla, V.F. Lysov, Honeycomb catalysts for clean-up of diesel exhausts based upon the anodic-spark oxidized aluminum foil, Catal. Today 53 (1999) 639–646.
[28] M.S. Vasil'eva, V.S. Rudnev, O.E. Sklyarenko, L.M. Tyrina, N.B. Kondrikov, Titanium-supported nickel–copper oxide catalysts for oxidation of carbon(II) oxide, Russ. J. Gen. Chem. 80 (2010) 1557–1562.
[29] M.S. Vasilyeva, V.S. Rudnev, I.S. Smirnov, An effect of heat processing on catalytic activity of a system MnOx, SiO2/TiO2/Ti, Russ. J. Appl. Chem. 86 (2013) 112–115.
[30] M.S. Vasilyeva, V.S. Rudnev, A.Yu. Ustinov, M.A. Tsvetnov, Formation, composition, structure, and catalytic activity in CO oxidation of SiO2 + TiO2/Ti composite before and after modification by MnOx or CoOx, Surf. Coat. Technol. 275 (2015) 84–89.
[31] I.V. Lukiyanchuk, V.S. Rudnev, I.V. Chernykh, I.V. Malyshev, L.M. Tyrina, M.V. Adigamova, Composites with transition metal oxides on aluminum and titanium and their activity in CO oxidation, Surf. Coat. Technol. 231 (2016) 433–438.
[32] M.S. Vasilyeva, V.S. Rudnev, A.Yu Ustinov, I.A. Korotenko, E.B. Modin, O.V. Voitenko, Cobalt-containing oxide layers on titanium, their composition, morphology, and catalytic activity in CO oxidation, Appl. Surf. Sci. 257 (2010) 1239–1246.
[33] M.S. Vasilyeva, V.S. Rudnev, F. Wiedenmann, S. Wybornov, T.P. Yarovaya, X. Jiang, Thermal behavior and catalytic activity in naphthalene destruction of Ce-, Zr- and Mn-containing oxide layers on titanium, Appl. Surf. Sci. 258 (2011) 719–726.
[34] X. Yu, Li Chen, Y. He, Z. Yan, In-situ fabrication of catalytic metal oxide films in microchannel by plasma electrolytic oxidation, Surf. Coat. Technol. 269 (2015) 30–35.
[35] J. Wang, Ch. Li, Zh. Yao, M. Yang, Y. Wang, Q. Xia, Zh. Jiang, Preparation of Fenton-like coating catalyst on Q235 carbon steel by plasma electrolytic oxidation in silicate electrolyte, Surf. Coat. Technol. 307 (2016) 1315–1321.
[36] J. Wang, Zh. Yao, Q. Xia, Y. Wang, Zh. Jiang, A novel solid acid coating catalyst on Q235 carbon steel for Fenton-like oxidation of phenol under circumneutral pH, J. Alloys Compd. 711 (2017) 278–286.
[37] J. He, Q. Luo, Q.Z. Cai, X.W. Li, D.Q. Zhang, Microstructure and photocatalytic properties of WO3/TiO2 composite films by plasma electrolytic oxidation, Mater. Chem. Phys. 129 (2011) 242–248.
[38] N. Salami, M.R. Bayati, F. Golestani-Fard, H.R. Zargar, UV and visible photodecomposition of organic pollutants over micro arc oxidized Ag-activated TiO2 nanocrystalline layers, Mater. Res. Bull. 47 (2012) 1080–1088.
[39] H.-J. Oh, Ch.-S. Chi, Eu–N-doped TiO2 photocatalyst synthesized by micro-arc oxidation, Mater. Lett 86 (2012) 31–33.
[40] X. Wu, Q. Wei, J. Zhaohua, Influence of Fe3+ ions on the photocatalytic activity of TiO2 films prepared by micro-plasma oxidation method, Thin Solid Films 496 (2006) 288–292.
[41] S. Petrović, S. Stojadinović, L.J. Rožić, N. Radić, R. Vasilić, Process modelling and analysis of plasma electrolytic oxidation of titanium for TiO2/WO3 thin film photocatalysts by response surface methodology, Surf. Coat. Technol. 269 (2015) 250–257.
[42] T. Soejima, H.S. Yagyu, Ito, One-pot synthesis and photocatalytic activity of Fe-doped TiO2 films with anatase–rutile nanojunction prepared by plasma electrolytic oxidation, J. Mater. Sci. 46 (2011) 5378–5384.
[43] V.I. Chernenko, L.A. Snezhko, I.I. Papanva, Fabrication of Coatings by Anode-Spark Electrolysis, Khimia Leningrad, 1991 (In Russian).
[44] I.V. Suminov, P.N. Belkin, A.V. Epel'feI'd, V.B. Lyudin, B.L. Krit, A.M. Borisov, Plazmenno-elektroliticheskoe Modifitsirovanie Poverkhnosti Metallov I Splavov (Plasma Electrolytic Surface Modification of Metals and Alloys), Tekhnosfera, Moscow, 2011 (In Russian).
[45] M.S. Vasilyeva, A.P. Artemyanov, V.S. Rudnev, N.B. Kondrikov, The porous structure of silicon-containing surface layers formed on titanium by plasma-electrolytic, Prot. Met. Phys. Chem. Surf. 50 (2014) 499–507.
[46] V.L. Singleton, A. Rossi, Colorimetry of total phenolics with phosphomolybdic-phosphotungstic acid reagents, Am. J. Enol. Vitic. 16 (1965) 144–158.
[47] R.M. Cornell, U. Schwertmann, The Iron Oxides: Structure, Properties, Reactions, Occurrences, and Uses, Wiley, Weinheim, Germany, 2003.
[48] M. Aizawa, Y. Nosaka, N. Fujii, FT-IR liquid attenuated total reflection study of TiO2-SiO2 sol-gel reaction, J. Non-Cryst. Solids 128 (1991) 77–85.
[49] E.B. Burgina, G.N. Kustova, S.V. Tsybulya, G.N. Kryukova, G.S. Litvak, L.A. Isupova, V.A. Sadykov, Structure of the metastable modification of iron(III) oxide, J. Struct. Chem. 41 (2000) 396–402.
[50] Y. Wang, J. Fang, J.C. Crittenden, C. Shen, Novel RGO/ α-FeOOH supported catalyst for Fenton oxidation of phenol at a wide pH range using solar-light-driven irradiation, J. Hazard. Mater. 329 (2017) 321–329.
[51] R. Matta, K. Hanna, S. Chiron, Fenton-like oxidation of 2,4,6-trinitrotoluene using different iron minerals, Sci. Total Environ. 385 (2007) 242–251.
[52] A.C. da Silva, M.R. Almeida, M. Rodriguez, A.R.T. Machado, L.C.A. de Oliveira, M. C. Pereira, Improved photocatalytic activity of ≏-FeOOH by using H2O2 as an electron acceptor, J. Photochem. Photobiol. B. 332 (2017) 54–59.
[53] J. Feng, X. Hu, P.L. Yue, Discoloration and mineralization of Orange II using different heterogeneous catalysts containing Fe: a comparative study, Environ. Sci. Technol. 38 (2004) 5773–5778.
[54] B. Yuan, X. Li, K. Li, W. Chen, Degradation of dimethyl phthalate (DMP) in aqueous solution by UV/Si–FeOOH/H2O2, Colloids Surf. A 379 (2011) 157–162.
[55] A.R. Khataee, A. Khataee, M. Fathinia, Y. Hanifehpour, S.W. Joo, Kinetics and mechanism of enhanced photocatalytic activity under visible light using synthesized PrxCd1–xSe nanoparticles, Ind. Eng. Chem. Res. 52 (2013) 13357–13369.
[56] R. Crutescu, C. Ungureanu, Aspects regarding the kinetics of phenols degradation by Pseudomonas putida, Rev. Chim. (Bucharest) 58 (2007) 1322–1326.
[57] A.N. Soon, B.H. Hameed, Heterogeneous catalytic treatment of synthetic dyes in aqueous media using Fenton and photo-assisted Fenton process, Desalination 269 (2011) 1–16.